Trace gas fluxes from tidal salt marsh soils: implications for carbon-sulfur biogeochemistry

Margaret Capooci[1] and Rodrigo Vargas [1]

[1] Department of Plant and Soil Science
University of Delaware
152 Townsend Hall
531 South College Ave.
Newark, DE, USA 19716

Correspondence to:
Rodrigo Vargas
152 Townsend Hall
531 South College Ave.,
Newark, DE 19716
rvargas@udel.edu
Phone: 302-831-1386

Abstract

Tidal salt marsh soils can be a dynamic source of greenhouse gases such as carbon dioxide (CO_2), methane (CH_4), and nitrous oxide (N_2O), as well as sulfur-based trace gases such as carbon disulfide (CS_2) and dimethylsulfide (DMS) which play roles in global climate and carbon-sulfur biogeochemistry. Due to the difficulty in measuring trace gases in coastal ecosystems (e.g., flooding, salinity), our current understanding is based on snap-shot instantaneous measurements (e.g., performed during daytime low tide) which complicates our ability to assess the role of these ecosystems for natural climate solutions. We performed continuous, automated measurements of soil trace gas fluxes throughout the growing season to obtain high-temporal frequency data and to provide insights into magnitudes and temporal variability across rapidly changing conditions such as tidal cycles. We found that soil CO_2 fluxes did not show a consistent diel pattern, CH_4, N_2O, and CS_2 fluxes were highly variable with frequent pulse emissions (>2,500%, >10,000%, and >4,500% change, respectively), and DMS fluxes only occurred mid-day with changes >185,000%. When we compared continuous measurements with discrete temporal measurements (during daytime, at low tide), discrete measurements of soil CO_2 fluxes were comparable with those from continuous measurements, but misrepresent the temporal variability and magnitudes of CH_4, N_2O, DMS, and CS_2. Discrepancies between the continuous and discrete measurement data result in differences for calculating the sustained global warming potential (SGWP), mainly by an overestimation of CH_4 fluxes when using discrete measurements. The high temporal variability of trace gas fluxes complicates the accurate calculation of budgets for use in blue carbon accounting and earth system models.

1. Introduction

Coastal vegetated ecosystems such as tidal salt marshes, mangrove forests, and seagrass beds provide a wide range of ecosystem services, such as mitigating storm surge and providing nursery areas for fish species (Barbier et al., 2011; Möller et al., 2014). They also can potentially store large amounts of carbon at rates forty times higher than tropical rainforests (Rosentreter et al., 2018; Duarte et al., 2005) and are referred to as "blue carbon" ecosystems. The importance of coastal vegetated ecosystems in climate change policies has been recognized by the Paris Agreement (UNFCCC, 2015). Prior to the Paris Agreement, there has been increased interest in better quantifying the net balance between carbon storage and carbon release in coastal vegetated ecosystems for both scientific and carbon market purposes. For example, the Verified Carbon Standard developed a methodology to assess and verify the amount of carbon removed from the atmosphere in tidal wetland and seagrass restoration projects for carbon market purposes (Emmer et al., 2021). However, there are major knowledge gaps in assessing blue carbon in coastal vegetated ecosystems. Specifically, the high spatial and temporal variability of greenhouse gas (GHG) emissions, particularly for CH_4 and N_2O, in coastal vegetated ecosystems complicates blue carbon offset calculations (Rosentreter et al., 2021; Capooci et al., 2019; Al-Haj and Fulweiler, 2020; Murray et al., 2015). Thus, there is a need for developing measurement protocols to fully quantify the contribution of multiple GHGs in blue carbon ecosystems.

To improve our understanding of blue carbon ecosystems in global biogeochemical cycles we need to think beyond traditional GHG trace gases (i.e., CO_2, CH_4, N_2O). Tidal salt marshes produce sulfur-based trace gases due to the prevalence of sulfur cycling within their soils, which has implications for carbon-sulfur biogeochemistry and the global climate. While coastal areas are major sources of sulfur gases (Kellogg et al., 1972), there is large

65 uncertainty in emission rates (Carroll et al., 1986; Andreae and Jaeschke, 1992; Brimblecombe,

66 2014). Dimethyl sulfide (DMS) is one of the dominant sulfur-based gases emitted from salt

67 marshes (Hines, 1996) and is considered a climate cooling gas, in part due to its oxidation to SO_4

68 in the atmosphere (Thomas et al., 2010; Watts, 2000; Charlson et al., 1987).

69 Dimethylsulfoniopropionate (DMSP), a DMS precursor, can be produced by salt marsh plant

70 species *Spartina alterniflora*, *S. anglica*, and *S. foliosa* (Hines, 1996). DMS plays an important

71 role in linking together carbon and sulfur biogeochemistry in salt marsh soils. It can be

72 decomposed by not only sulfate-reducing bacteria, but can also act as a non-competitive

73 substrate for methylotrophic methanogenesis (Kiene, 1988; Kiene and Visscher, 1987; Oremland

74 et al., 1982) which allows methane production to occur in soils dominated by sulfate reduction

75 (Seyfferth et al., 2020). Another sulfur-based trace gas released from tidal salt marshes is carbon

76 disulfide (CS_2), which has an insignificant global warming potential and a short atmospheric

77 lifetime (Brühl et al., 2012). However, CS_2 is a precursor to carbonyl sulfide (COS; Whelan et

78 al., 2013). COS is the most abundant reduced sulfur compound in the atmosphere and can form

79 sulfate aerosols that affect the Earth's radiative properties by reflecting sunlight, thereby having

80 a cooling effect on the climate (Watts, 2000; Taubman and Kasting, 1995). Despite sulfur-based

81 trace gases playing a role in wetland soil biogeochemistry and in global climate, there is a need

82 to quantify coastal wetland sulfur emissions and to connect those emissions to both the salt

83 marsh sulfur cycle and to global budgets (DeLaune et al., 2002; Whelan et al., 2013).

84   Historically, both soil GHGs and S-based fluxes are measured using manual survey

85 chambers, particularly during daytime low tide (e.g., De Mello et al., 1987) when soils are less

86 likely to be submerged and are accessible to researchers. Measurements at high tide in salt

87 marshes are difficult due to both reduced access to the marsh platform and reduced fluxes. Gases

88   from the soil mix with the overlying water column and move more slowly through water

89   compared to air, contributing to a decline in fluxes during high tide (Moffett et al., 2010).

90   Manual measurements have a number of advantages, including the ability to sample over large

91   areas over short periods of time (Moseman-Valtierra et al., 2016; Simpson et al., 2019), but these

92   measurements are labor-intensive and provide limited information regarding temporal variability

93   (Koskinen et al., 2014; Savage et al., 2014; Vargas et al., 2011). On the other hand, recent

94   advances in high temporal-frequency soil efflux measurements (Capooci and Vargas, 2022;

95   Diefenderfer et al., 2018; Järveoja et al., 2018) have provided researchers with unprecedented

96   temporal information to better understand diel and tidal patterns, as well as the influence of pulse

97   events on trace gas emissions within salt marshes. While the use of automated systems is

98   becoming more common in measuring salt marsh fluxes (Capooci and Vargas, 2022;

99   Diefenderfer et al., 2018; Trifunovic et al., 2020), their use is limited by high instrumentation

100   costs, electricity requirements, and logistical challenges associated with installing these

101   instruments in an environment prone to flooding and with high humidity. As automated systems

102   become more prevalent, it provides researchers with the opportunity to evaluate data collected

103   from manual measurements, such as daily means, that have been used to inform models and

104   budgets, particularly for understudied trace gases such as N_2O, CS_2, and DMS.

105   The objective of this study is to characterize the spatial and temporal variability of trace

106   gases from soils in a tidal salt marsh. Specifically, we focus on CO_2, CH_4, N_2O, CS_2, and DMS

107   to assess the differences between measurements taken at a particular time of day (i.e., daytime

108   low tide) and measurements with high-temporal frequency (i.e., continuous hourly measurements

109   for ~72 hours). Few studies have measured GHG fluxes from tidal salt marshes using

110   continuous, automated measurements (Diefenderfer et al., 2018; Capooci and Vargas, 2022), and

111   this is a pioneering study that provides unprecedented information about the magnitudes and

112   patterns of CS_2 and DMS fluxes via continuous measurements. Furthermore, this study tests

113   whether traditional measurement protocols based on discrete temporal measurements provide

114   similar information as data derived from continuous measurements, including the calculation of

115   the sustained global warming potential (SGWP). Development of new technologies and

116   incorporation of this information has important implications for calculating greenhouse and trace

117   gas budgets, as well as the role salt marshes play in global biogeochemical cycles.

118

119   **2. Materials and methods**

120

121   *2.1 Study site*

122   The study was conducted at St. Jones Reserve, the brackish estuarine component of the

123   Delaware National Estuarine Research Reserve. The site is part of the Delaware Estuary and is

124   tidally connected to the Delaware Bay via the St. Jones River. St. Jones is classified as a

125   mesohaline tidal salt marsh (DNREC, 1999) and has silty clay loam soils (10% sand, 61% silt,

126   29% loam, Capooci et al 2019). The study was conducted in a section of the marsh dominated by

127   *Spartina alterniflora* (= *Sporobolus alterniflorus* (Loisel.); Peterson et al., 2014) and will be

128   referred to as SS as established in previous studies (Seyfferth et al., 2020; Capooci and Vargas,

129   2022). This area is lower in elevation relative to the rest of the marsh, is characterized by sulfur

130   reduction (Seyfferth et al., 2020), and covers ~66% of the salt marsh landscape (Vázquez-Lule

131   and Vargas, 2021). The SS site rarely floods during high tide due to its distance from the tidal

132   creek (~50 m), as well as the presence of a berm located adjacent to the tidal creek (Seyfferth et.,

133   2020; Hill et al., 2021).

134

135 *2.2 Experimental set-up*

136   The experiment was performed over the course of 6 campaigns to cover a full growing

137 season: greenup (G), maturity (M), senescence (S), and dormancy (D) as described by the

138 canopy phenology of the study site (Hill et al., 2021). The campaigns began during the latter half

139 of the 2020 growing season and continued into beginning of the 2021 growing season (M1 – 29

140 June to 2 July, M2 – 31 July to 3 Aug, S1 – 31 Aug to 3 Sept, S2 – 28 Sept to 1 Oct, D1 – 13

141 Apr to 16 Apr, and G1 – 31 May to 3 June) due to delays related to the COVID-19 pandemic.

142 We installed six PVC collars (diameter: 20 cm), placed ~1.2 meters apart, four months prior to

143 the beginning of the experiment in the year 2020. Collars were placed in a *S. alterniflora* area of

144 the marsh near the boardwalk to minimize impacts to the marsh, as well as to easily access

145 boardwalk power outlets. Any vegetation that grew inside these collars in between campaigns

146 was carefully clipped at the base of the stem prior to each campaign. Vegetation was clipped on a

147 frequent basis to minimize stem diameters and thereby reduced the effects of plant-mediated gas

148 transport. These collars were used to set down six opaque automated chambers (LICOR 8100-

149 104, Lincoln, Nebraska; volume: 4071.1 cm^3) to measure trace gas fluxes as described below.

150

151 *2.3 Trace gas flux measurements and QA/QC*

152   The autochambers were coupled with a closed-path infrared gas analyzer (LI-8100A,

153 LICOR, Lincoln, Nebraska) and a Fourier transform infrared spectrometer (DX4040, Gasmet

154 Technologies Oy, Vantaa, Finland). The LI-8100A and the DX4040 were connected in parallel

155 since the DX4040 has its own internal pump and flow rates. Trace gas fluxes were measured

156 once per hour per chamber (i.e., all six chambers were measured within an hour). Measurements

157   were 5 minutes long and each chamber was flushed for 5 minutes total (pre-purge and post-purge

158   were both 2.5 minutes long) to help reduce the impacts of humidity on the instruments. Each

159   campaign lasted approximately 72 hours where approximately 416 measurements were recorded.

160   Campaigns were short in length due to electrical power limitations and to minimize

161   instrumentation damage due to the corrosive environmental conditions.

162   At the beginning of each campaign and every 24 hours after, we performed a zero

163   calibration on the DX4040 using ultra-pure 99.999% N_2 gas. It is recommended that zero

164   calibrations are performed every 24 hours and when the ambient temperature changes by 10°C,

165   so the experiment was paused for ~30 minutes during the zero calibrations each day. Gas fluxes

166   were calculated using Soil Flux Pro (v4.2.1, LICOR, Lincoln, Nebraska) and underwent

167   standardized quality assurance and quality control protocol as established in previous

168   publications (Capooci et al., 2019; Petrakis et al., 2017). QA/QC included several steps. First, all

169   values due to instrumental errors such as an insufficient chamber closure seal were removed.

170   These errors were identified by the SoilFluxPro software. Second, the R^2 for the linear and

171   exponential fits of trace gas emissions were compared and the fit with the higher R^2 was chosen.

172   Third, all fluxes that occurred when the R^2 of CO_2 was <0.90 were removed. Low R^2's indicate

173   that the soil micrometeorological conditions were not stable during the measurement. Finally, all

174   negative CO_2 fluxes were removed since they were likely erroneous.

175

176   *2.4 Ancillary measurements*

177   Meteorological (station: delsjmet-p) and water quality (station: Aspen Landing) data were

178   obtained from the National Estuarine Research Reserve's Centralized Data Management Office

179   (CDMO) and collected according to their protocol (System-wide Monitoring Program).

180   Meteorological data was collected using a CR1000 Meteorological Monitoring Station

181   (Campbell Scientific, Logan, UT, USA). Water quality data were measured using a YSI 6600

182   sonde (YSI Inc., OH, USA). Both data sets were cleaned and gap-filled following the protocol

183   established in Capooci et. al. (2022).

184   Phenological data were obtained from the PhenoCam network (site: stjones,

185   Seyednasrollah et al., 2019) as described previously (Trifunovic et al., 2020; Hill et al., 2021).

186   Briefly, a single mid-day photo (12:00:00 h) was selected for each of the days in the study period

187   and was visually inspected to remove images with obvious distortions. Since the images included

188   a variety of vegetation types, the region of interest delineated to only the area containing *S.*

189   *alterniflora*, the main species at the study site. Then the phenopix R package (Filippa et al.,

190   2020) was used to extract and calculate the greenness index, as well as delineate the phenophases

191   for the study period (Hill et al., 2021).

192

193   *2.5 Data analyses*

194   Daily averages and associated standard deviations were calculated for meteorological and

195   water quality data, except for the greenness index. Soil trace flux data were averaged into hourly

196   and daily means and standard deviations. For heat maps, average hourly and campaign-length

197   coefficients of variation were calculated.

198   We extracted measurements from the time series of the automated measurements to

199   represent information collected from discrete temporal measurements conducted during daytime

200   low tide. This approach aimed to represent a measurement protocol derived from manual (i.e.,

201   survey) measurements where most measurements are performed at daytime and low tide for

202   logistical reasons. To identify and extract these measurements, we identified when low tide

203 occurred during each day (between 9:00:00 and 17:00:00 h) of the campaigns from water level

204 data obtained from the tidal creek. All automated measurements that fell between 1 hour before

205 and 1 hour after low tide were extracted, averaged into a daily value, and classified as "discrete"

206 measurements. For example, if low tide fell at 13:00:00 h, all continuous measurements that fell

207 between 12:00:00 and 14:00:00 h were then extracted and averaged to obtain a daily mean. Daily

208 means were also calculated for all automated measurements collected during the day and will be

209 referred to as the "continuous" daily mean. Differences in the means and distributions of the

210 continuous and discrete fluxes were assessed using a t-test and a Kolmogorov-Smirnov test,

211 respectively.

212   Sustained global warming potential (SGWP) was calculated for both the campaign-long

213 and daytime low tide fluxes for CO_2, CH_4, and N_2O. SGWP accounts for sustained gas emissions

214 over time compared to the global warming potential which accounts for a pulse emission over

215 time (Neubauer and Megonigal, 2019). To calculate the SGWP, data from Day 2 and 3 of each

216 campaign was used since measurements on Day 1 and 4 did not always occur during daytime

217 low tide. Fluxes were converted into g m^{-2} and multiplied by the 20 and 100-year SGWP

218 (Neubauer and Megonigal, 2019). SGWP were compared to see whether extrapolating SGWP

219 from daily-averaged manual measurements done at low tide yielded similar values as hourly-

220 averaged from high temporal frequency measurements.

221

222 **3. Results**

223

224 *3.1 Meteorological and water quality*

225   Air temperature and greenness index show traditional seasonal patterns of temperate salt

226   marshes (Fig. 1). Daily mean air temperature ranged from -3.5°C to 29.9°C, with an average

227   daily temperature of 13.8 ± 9.1°C, while greenness index ranged from 0.30 to 0.42 with an

228   average of 0.34 ± 0.04. Relative humidity, barometric pressure, water level, and salinity varied

229   throughout the year. Relative humidity ranged from 32.6% to 100% with an average of 79.1% ±

230   16.7%. Barometric pressure was between 999.7 and 1036 mb with an average value of 1018.3 ±

231   6.8 mb. Daily water level ranged from -0.30 m to 0.76 m with an average height of 0.25 ± 0.2 m,

232   while salinity ranged from 1.1 ppt to 20.4 ppt with an average of 8.0 ± 4.45 ppt.

233

234
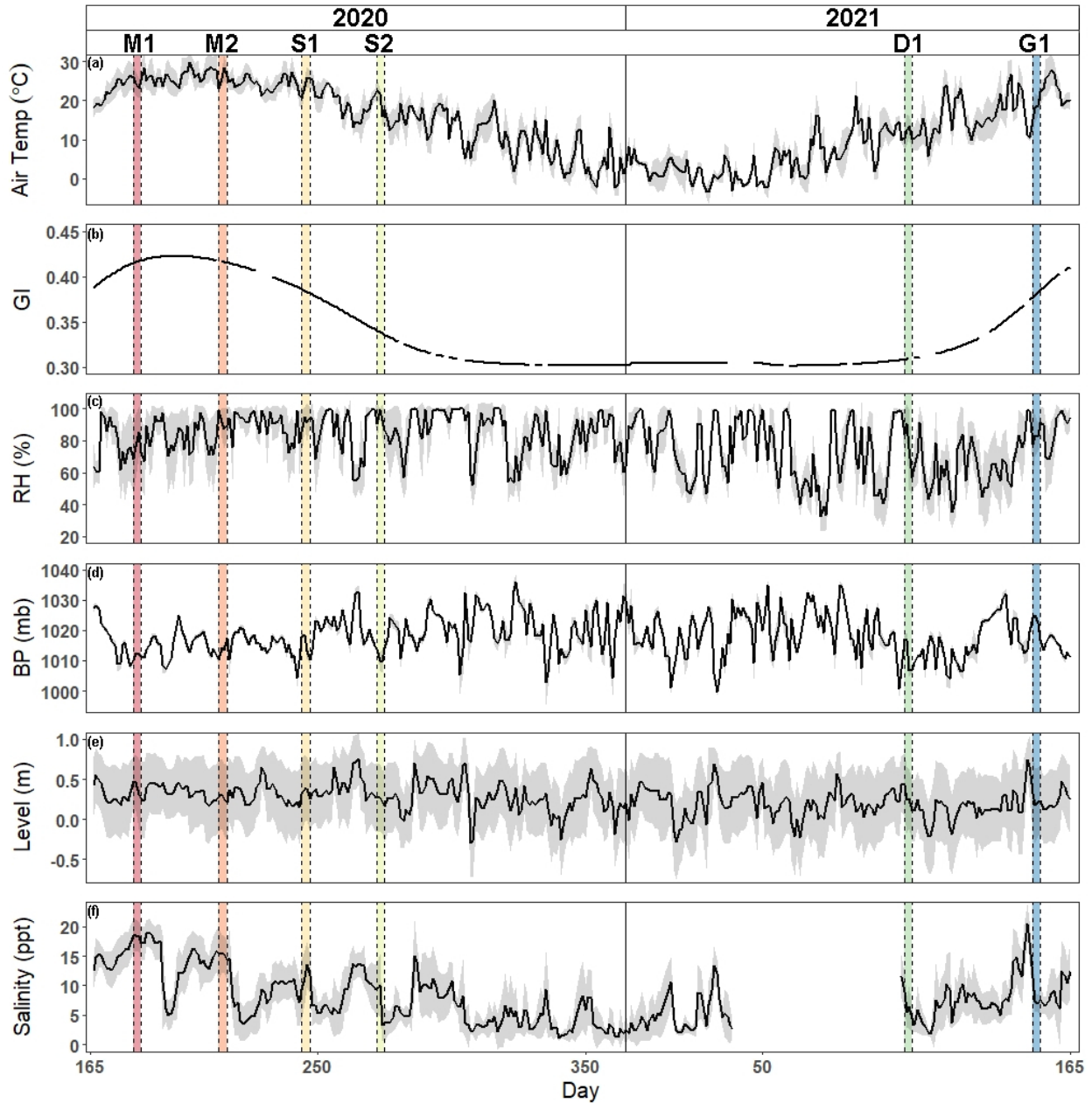
235 **Figure 1.** Time series of hourly mean ± SD (gray shaded region of (a) air temperature, (b)

236 greenness index, (c) relative humidity, (d) barometric pressure, (e) water level, and (f) salinity

237 from June 14, 2020 to June 14, 2021. Vertical shaded areas correspond to each of the campaigns

238 (M = maturity, S = senescence, D = dormancy, G = greenup).

239

240

3.2 Greenhouse gas and sulfur-based trace gas patterns and variability

Average CO_2 fluxes were significantly different in each campaign, with the highest average fluxes occurring during the G1 campaign and the lowest during the D1 campaign (Fig. 2a). During some campaigns, such as S1, CO_2 fluxes did not show similar temporal patterns between chambers, whereas during other campaigns, such as M2 and G1, all six chambers had similar patterns. While there is a seasonal pattern in CO_2 fluxes, with higher fluxes occurring during warmer months, diel patterns were not consistent between campaigns. One notable exception is the G1 campaign, during which a clear diel pattern was observed. CO_2 fluxes had consistent variability from one hour to the next during each of the 6 campaigns (Fig. 3a), with overall average variability ranging from 28.9% during M2 to 49.6% during Dl.

CH_4 fluxes were low most of the time, particularly during the G1 campaign (Fig. 2b). However, CH_4 pulses occurred during 5 out of the 6 campaigns, with S1and S2 having the most frequent pulse emissions. S2 had the largest CH_4 pulse,13,488 nmol m^{-2} s^{-1}, which was 2,599% higher than the average flux. The highest average CH_4 fluxes also occurred during S1 and S2, while the highest hourly variability occurred in both S1 and S2, as well as in M2 (Fig. 3b). Mean CH_4 variability ranged from -108% in M1 to 91.0% in S1.

Most N_2O fluxes were near-zero, with periodic pulses of emissions or uptake that ranged from -33.8 to 19.0 nmol m^{-2} s^{-1} (Fig. 2c), with a maximum percent change from the mean of 10,231%. Four out of the six campaigns (M1, S2, D1, and G1) had net N_2O uptake, while two campaigns (M2, S1) had net N_2O fluxes. There were no significant differences between campaigns except for M1 and S1. Meanwhile, N_2O fluxes had very high hourly variability ranging from -106,964% to 26,208% (Fig. 3c). Consequently, average variability during each campaign was highly variable from -1,032% to 129%.

264   Similarly to CH_4 and N_2O, CS_2 fluxes were low the majority of the time, with occasional

265   pulses of emissions or uptake (Fig. 2d). CS_2 fluxes ranged from -386.9 to 306.2 nmol m^{-2} s^{-1},

266   with a maximum percent change from the mean of 4,785%. All campaigns had net emissions

267   despite periodic pulses of CS_2 uptake. CS_2 fluxes also had high hourly variability, with overall

268   means for each campaign ranging from -70.2% during D1 to 2254% during M2 (Fig. 3d).

269   DMS emissions were zero for most of the campaigns (Fig. 2e). Pulses of emissions and

270   uptake tended to occur during mid-day. DMS fluxes ranged from -158.5 to 230 nmol m^{-2} s^{-1},

271   with a maximum percent change from the mean of 185,987%. D1 and G1 had net uptake, while

272   the other four campaigns had net emissions of DMS. During periods of emissions and uptake,

273   hourly variability ranged from -870.5% to 888.7% (Fig. 2e). The extended periods of no DMS

274   fluxes contributed to low overall mean variability during each campaign, ranging from -2.45% in

275   S2 to 35.7% in M2.

276

277

Figure 2. Time series of fluxes from each chamber during each campaign for (a) CO_2, (b) CH_4,

(c) N_2O, (d) CS_2, and (e) DMS. Each color designates a different chamber. The campaign means

[LCI = lower 95% confidence interval, UCI = upper 95% confidence interval] are listed on each

panel. The y-axis for CH_4 fluxes was shortened to show the variability. Full range of CH_4 fluxes

during S2 can be seen in Supplementary Figure (SF) 1.

283
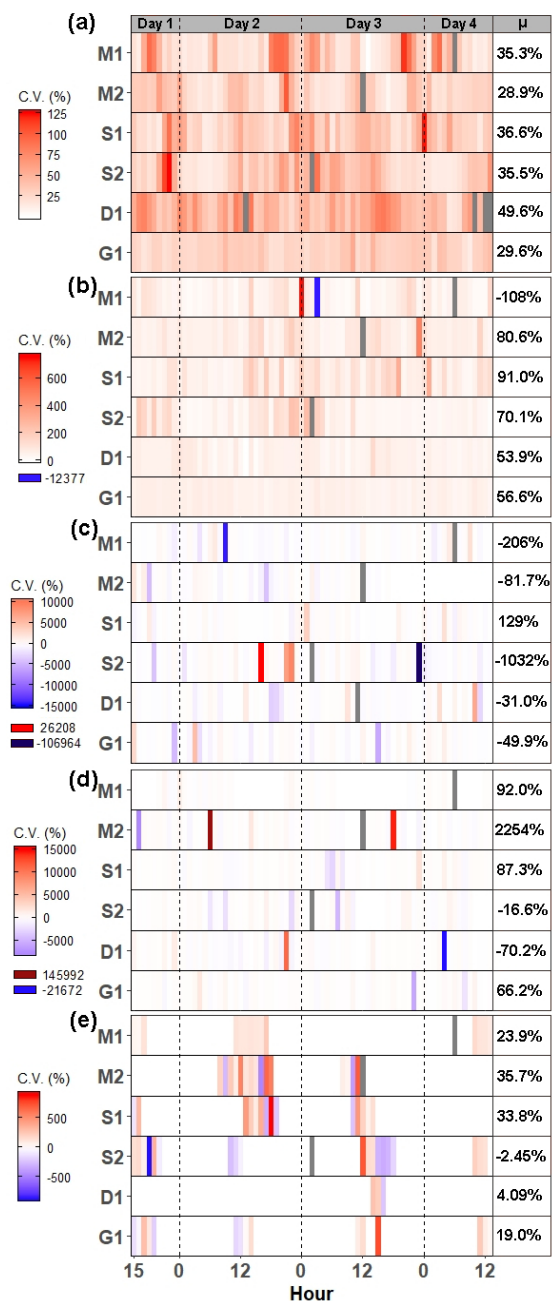
Figure 3. Heat maps of hourly coefficient of variance (CV) for (a) CO_2, (b) CH_4, (c) N_2O, (d) CS_2, and (e) DMS during each campaign. Each pixel represents the average CV for that hour. Mean CV for each campaign is listed in the μ column. Grayed out pixels represent NA. Note: legend scale is different for each gas and campaigns start at 15:00:00 h on Day 1 and end at 13:00:00 h on Day 4.

289   *3.3 Comparisons between continuous and discrete measurement scenarios*

290   A subset of the continuous measurements that fall during daytime low tide was selected

291   to represent data collected using traditional discrete, manual measurements which are commonly

292   reported for tidal salt marshes. Information from continuous and discrete datasets are compared

293   to elevate whether they provide similar distributions, daily means, flux-temperature

294   relationships, and SGWP.

295   Continuous and discrete flux distributions can be seen via density plots (Fig. 4). While

296   the distributions for continuous and discrete fluxes overlap for each of the five gases, four of the

297   five gases have significantly different distributions of fluxes when comparing the continuous and

298   the discrete datasets (Table 1). The only gas that had similar distributions between the two

299   sampling intervals was CO_2 (Table 1). For all gases, the continuous distribution had higher

300   kurtosis values and higher C.V. than the discrete fluxes (Table 1). Of the five gases, CS_2 was the

301   only one with a more skewed discrete data distribution and significantly different means between

302   continuous and discrete measurement scenarios (Fig. 4b, Table 1).

303   For CS_2 and DMS, discrete measurements had higher overall daily mean fluxes (Fig. 5d,

304   5e), while the opposite occurred for CH_4 and N_2O (Fig. 5b, 5c). CO_2 fluxes from continuous and

305   discrete measurements had nearly a 1:1 relationship (Fig. 5a). Both CO_2 and DMS had strong

306   relationships between continuous and discrete daily means, with r-squares higher than 0.7, while

307   N_2O and CS_2 had moderate relationships. CH_4 had a poor fit between continuous and discrete

308   measurements.

309   Next, relationships between trace gas flux and air temperature were evaluated for each

310   gas under continuous and discrete measurement scenarios. CO_2 and CH_4 fluxes had statistically

311   significant relationships for both discrete and continuous measurements versus air temperature

312   (Fig. 6a-d). Air temperature explained 38% and 21% of the variability for discrete and

313   continuous measurements for CO_2, respectively (Fig. 6a, b), while air temperature explained

314   32% and 7% of the variability for discrete and continuous measurement for CH_4 (Figs. 6c, d).

315   The slopes for both discrete and continuous CO_2 fluxes were not significantly different (95% CI;

316   0.029 - 0.12, 0.037 - 0.054, respectively), as well as for CH_4 (95% CI; 2.14 - 12.7, 1.31 - 2.71,

317   respectively). For N_2O, CS_2, and DMS, there were no significant relationships between discrete

318   daily mean fluxes and air temperature, but there were significant relationships between

319   continuous hourly mean fluxes and air temperature (Fig. 6e-j). Air temperature explained very

320   little variability for N_2O, CS_2, and DMS.

321   Discrete measurements had a higher SGWP potential than the continuous measurements

322   (Table 2). While the discrete measurements had a slightly lower SGWP for CO_2 and a slightly

323   higher SWGP for N_2O, the difference between continuous and discrete SGWP was driven by

324   CH_4. The 20-yr and 100-yr SGWP for discrete measurements of CH_4 were up to ~38% higher

325   than the respective continuous measurements, contributing to an overall increase of ~18% and

326   ~11% for the discrete measurement's 20- and 100-year SGWP.

327

328
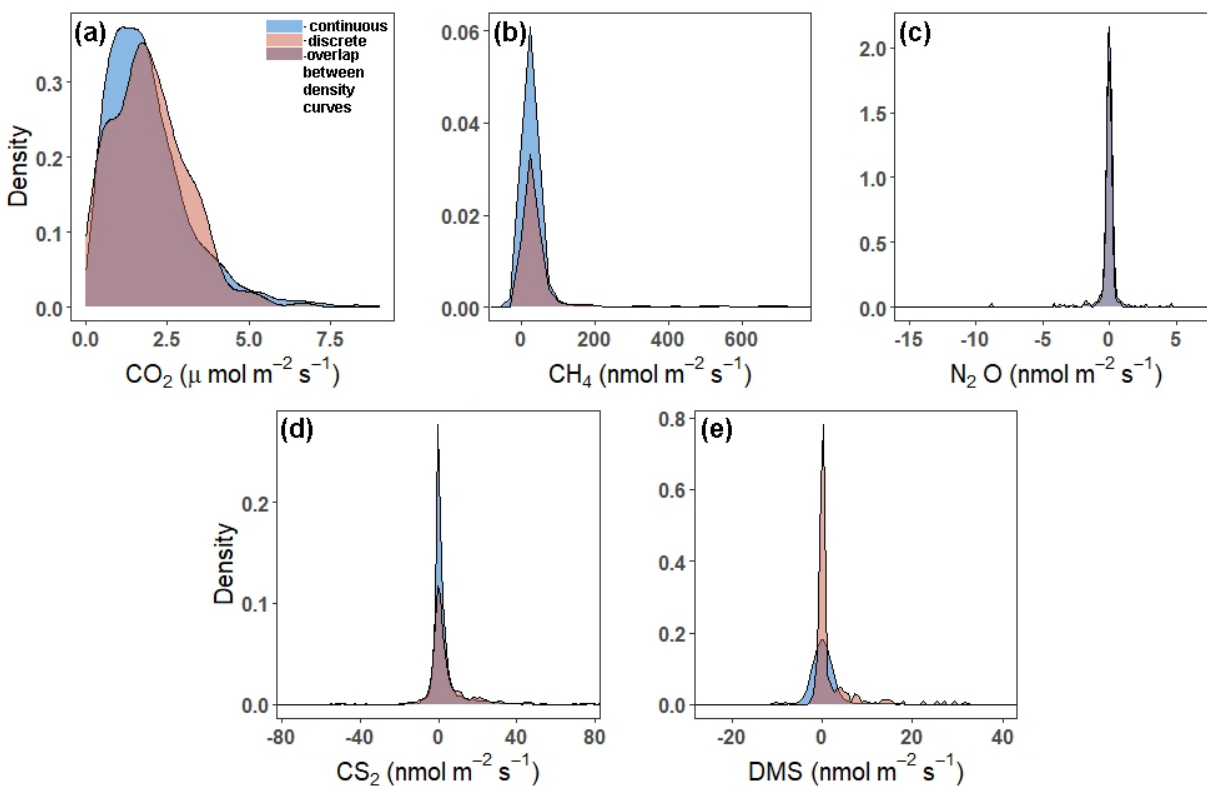
Figure 4. Density plots comparing the distribution of fluxes throughout all campaigns

(continuous over ~72 hours) to those measured during daytime low tide (discrete, one hour

before and one hour after daytime low tide) for (a) CO_2, (b) CH_4, (c) N_2O, (d) CS_2, and (e) DMS.

Note: The scales on the x- and y-axes are different. The tails have been cut off to better see the

peaks for (b), (c), (d), and (e). To see plots with full distributions, see SF 2.

334 **Table 1.** Summary of continuous (over ~72 hours) and discrete (one hour before and one hour

335 after low tide) measurement data and distributions for each gas. An alpha of < 0.05 was used to

336 determine significant differences between the means and the distributions. Note: Means for CO_2

337 are in $\mu mol\ m^{-2}\ s^{-1}$, while the other gases are in $nmol\ m^{-2}\ s^{-1}$.

338

Gas	Sampling Frequency	Mean	95% CI	C.V.	Skewness	Kurtosis	Means Different?	Distributions Different?
CO_2	Continuous	1.92	1.86–1.97	67.2%	1.53	6.51	No	No
	Discrete	1.90	1.74–2.07	62.3%	0.67	3.65		
CH_4	Continuous	41.2	29.5–52.9	708%	41.6	1903	No	Yes p = 0.02
	Discrete	57.6	39.2–76.0	234%	5.21	34		
N_2O	Continuous	-0.06	-0.13–0.009	2686%	-4.67	133	No	Yes p < 0.001
	Discrete	-0.16	-0.29--0.04	556%	-4.39	47.8		
CS_2	Continuous	3.39	2.45–4.33	673%	1.51	116	Yes p = 0.04	Yes p = 0.05
	Discrete	6.44	3.70–9.18	312%	3.93	22.9		
DMS	Continuous	1.11	0.70–1.51	907%	8.74	223	No	Yes p < 0.001
	Discrete	1.77	1.06–2.48	295%	3.40	16.6		

339

340

341
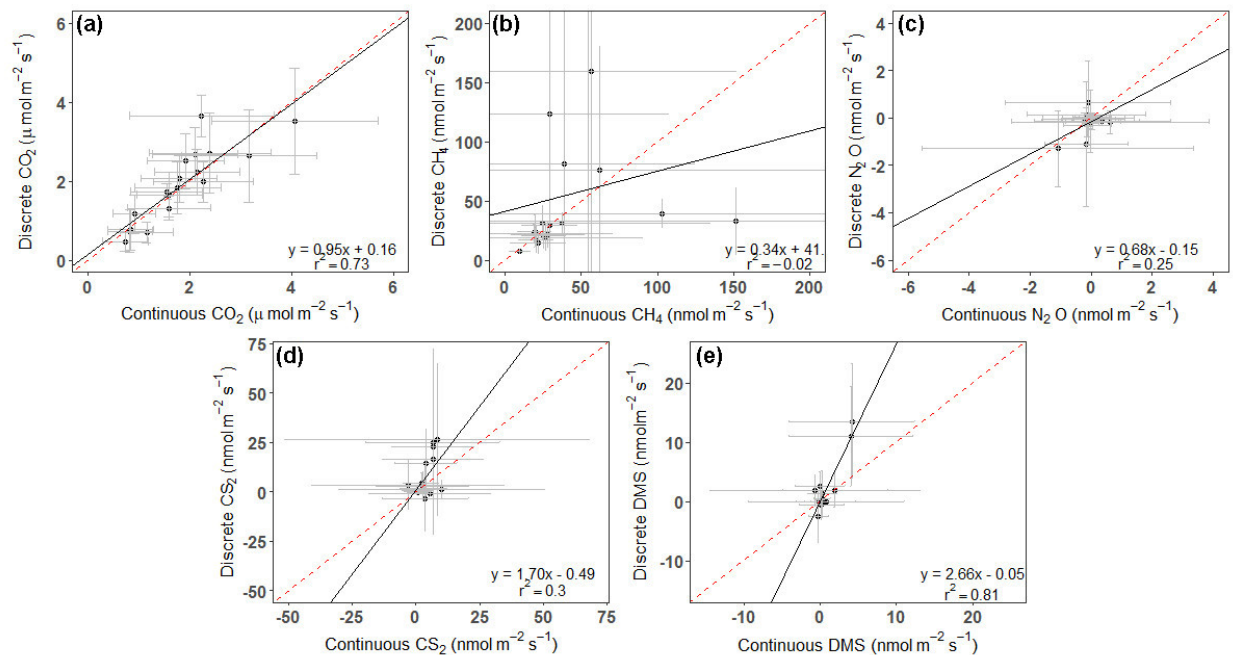
342 **Figure 5.** Plots comparing the daily average of continuous (over ~72 hours) to discrete (one hour

343 before and one hour after daytime low tide) measurements for (a) CO_2, (b) CH_4, (c) N_2O, (d)

344 CS_2, and (e) DMS. Error bars represent the SD and have been cut off in panel (b) to show data

345 better. See SF 3 for full error bars for panel b. Red dashed line is the 1:1 line, while the black

346 solid line is the trend line.

347
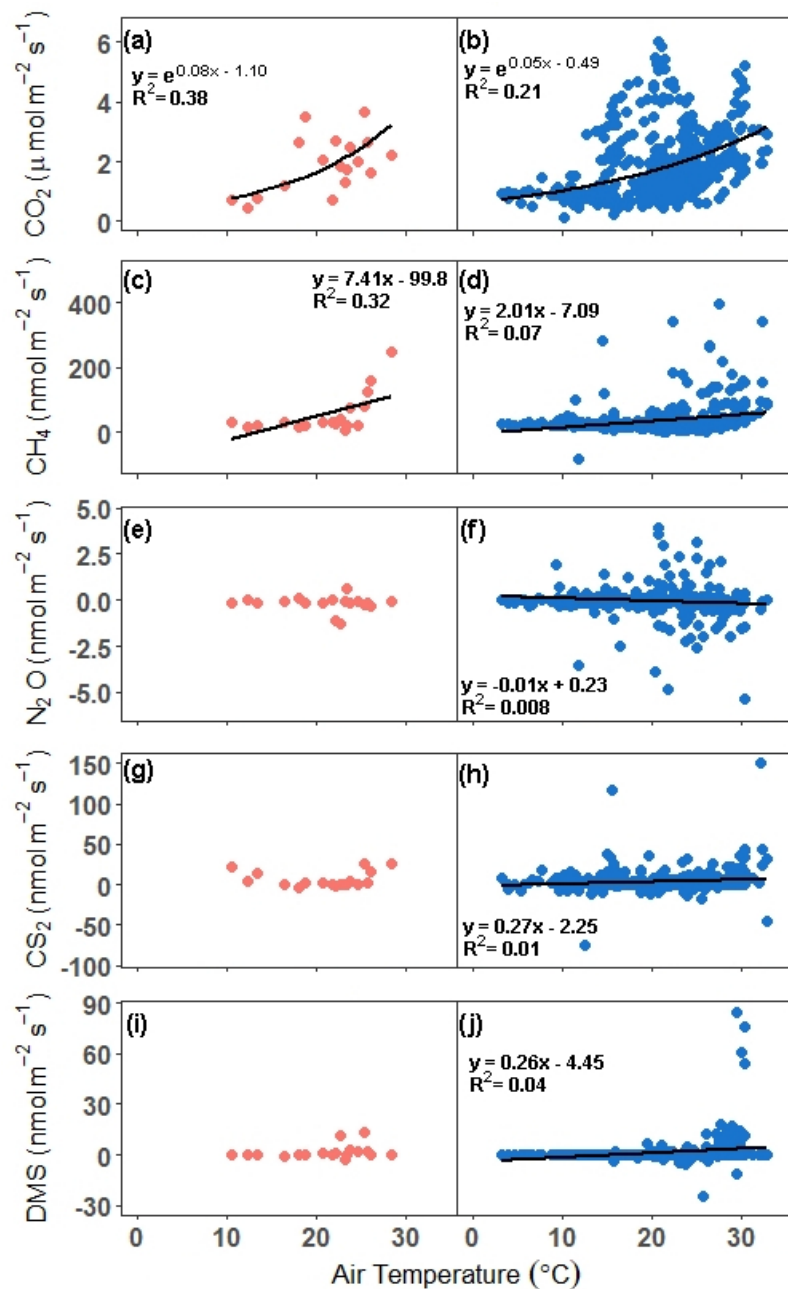
Figure 6. Comparison of fluxes versus air temperature for all campaigns. In panels, a, c, e, g, and

I, the hourly continuous (over ~72 hours) mean is compared to the hourly air temperature, while

in panels b, d, f, h, and k, the discrete (one hour before and one hour after daytime low tide) daily

mean is compared to the daily air temperature. The trend lines for significant relationships at

352 alpha <0.05 are plotted. Note: In panel d, the outlier hourly mean of 2,275 nmol m^{-2} s^{-1} is not

353 included in the trend line or in the graph.

354

355 **Table 2.** Sustained global warming potential (SGWP) derived from continuous (over ~72 hours)

356 and discrete (one hour before and one hour after daytime low tide) temporal measurements in a

357 tidal salt marsh.

358

Frequency	CO$_2$ (g m^{-2})	CH$_4$ (CO$_{2\text{-eq}}$ (g m^{-2}))		N$_2$O (CO$_{2\text{-eq}}$ (g m^{-2}))		Total (CO$_{2\text{-eq}}$ (g m^{-2}))	
		20-yr SGWP	100-yr SGWP	20-yr SGWP	100-yr SGWP	20-yr SGWP	100-yr SGWP
Continuous	84.9	70.4	33.0	0.27	0.30	155.57	118.2
Discrete	82.7	103.2	48.4	0.40	0.44	186.3	131.54

359

360

361 **4. Discussion**

362 *4.1 Measuring all the time: seasonal and diel patterns and hot moments of soil trace gases*

363   Spatial variability between the individual chambers at SS were low, but CO$_2$ fluxes

364 showed temporal variability that corresponded to changes in temperature. The relatively low

365 spatial variability within our experimental setting contrasts with previously reported high spatial

366 variability of CO$_2$ fluxes attributed to the presence of a hot spot (Capooci and Vargas, 2022).

367 However, previous CO$_2$ fluxes measured at the SS site ranged from 0-15 μmol m^{-2} s^{-1}, with the

368 bulk of the measurements between 0-5 μmol m^{-2} s^{-1}, with higher fluxes associated with hot spots

369 or warmer temperatures (Capooci and Vargas, 2022; Seyfferth et al., 2020; Hill and Vargas,

370 2022). Therefore, location of measurements within a landscape could be influenced by hot spots,

371   which complicates ecosystem scale calculations of soil CO_2 fluxes (Barba et al., 2018). In

372   addition, there was a seasonal pattern evident in the CO_2 fluxes, with higher emissions during the

373   growing season, as typical in temperate ecosystems, as well in the significant relationship

374   between CO_2 and air temperature. Within salt marshes, soil organic matter decomposition into

375   products such as CO_2 correlates with temperature due to the activation energy needed for organic

376   matter breakdown (McTigue et al., 2021). Other studies at temperate wetland sites have found

377   higher fluxes during the summer (Simpson et al., 2019; Yu et al., 2019; Bridgham and

378   Richardson, 1992), as well as relationships between CO_2 fluxes and temperature (Capooci and

379   Vargas, 2022; Simpson et al., 2019; Xie et al., 2014) highlighting that CO_2 fluxes in temperate

380   salt marshes exhibit a temperature dependency over seasonal scales, even in the presence of

381   tides.

382   While CO_2 fluxes show seasonal patterns, there are no diel patterns that persist

383   throughout the year. During G1, the peak of high tide coincided with peak daily temperature.

384   This scenario also occurred during D1, but fluxes were too low to discern patterns. During all

385   other campaigns, low tide and peak temperatures coincided. These results suggest that diel

386   patterns may occur periodically under certain conditions. For example, at the SS site, it may be

387   that diel patterns occur during high tide at the temperature peak. While we expected the highest

388   fluxes during low tides due to increased oxygen exposure, there may be a lag between low tide in

389   the creek and low water levels at the SS site, resulting in higher fluxes during high tide in the

390   creek. However, these results can vary from site to site and with proximity to the tidal creek.

391   More research using high temporal frequency measurements are needed to parse out the role of

392   temperature and tides on CO_2 fluxes across salt marshes to properly represent the pattern in earth

393   system models (Ward et al., 2020)

394   Similarly to CO_2, CH_4 has a significant relationship with air temperature, however it

395   explains less variability in the fluxes. Several studies have found positive correlations between

396   soil CH_4 fluxes and temperature (Bartlett et al., 1985; Emery and Fulweiler, 2014; Wang and

397   Wang, 2017) in temperate salt marshes, while others have not (Wilson et al., 2015). It is

398   important to note that while, in general, salt marsh CH_4 fluxes are positively related to

399   temperature (Al-Haj and Fulweiler, 2020), the ability of temperature to explain CH_4 flux

400   variability is low, compounded by many, often site-specific, factors that affect methane

401   production and consumption, such as organic matter supply, microbial communities, and

402   diffusion rates (Al-Haj and Fulweiler, 2020; Bartlett et al., 1985).

403   At our study site, CH_4 fluxes were highest and pulses were most frequent during

404   senescence, agreeing with findings from ecosystem-scale measurements derived using the eddy

405   covariance technique (Vázquez-Lule and Vargas, 2021). In most wetland ecosystems, including

406   those in northern, temperate, and subtropical areas, the highest fluxes have been reported during

407   the summer (Kim et al., 1998; Rinne et al., 2007; Van Der Nat and Middelburg, 2000; Livesley

408   and Andrusiak, 2012; Turetsky et al., 2014), but we highlight that there is a lack of

409   measurements during the winter (Al-Haj and Fulweiler, 2020). In *S. alterniflora* marshes, highest

410   mean CH_4 fluxes have been found in both the summer and the fall (Bartlett et al., 1985; Emery

411   and Fulweiler, 2014). At a site dominated by *S. alterniflora,* both high fluxes and porewater CH_4

412   concentrations were found in September (Zhang and Ding, 2011), indicating either a continual

413   build-up of CH_4 in the porewater over the growing season and/or increased CH_4 production in

414   the fall. For our site, it is likely higher CH_4 emissions during senescence were due to an input of

415   labile organic matter from plant die-off (Seyfferth et al., 2020). Furthermore, a recent study has

416   shown that porewater DMS, a non-competitive substrate for methylotrophic methanogenesis that

417   is produced from the breakdown of DMSP, a metabolite produced by *S. alterniflora* (Dacey et

418   al., 1987), peaks during the fall (Tong et al., 2018). Therefore, we postulate that an influx of

419   DMS may also contribute to higher CH_4 fluxes during senescence in marshes dominated by *S.*

420   *alterniflora*. This finding highlights the importance of carbon-sulfur biogeochemistry and

421   measuring fluxes during non-summer months; particularly in marshes that have plant

422   communities that provide substrates used in methylotrophic methanogenesis (Seyfferth et al.,

423   2020).

424   On a diel timescale, pulse emissions of CH_4 from the soil tend to occur during the

425   warmest time of the day, as well as during low and rising tides. There are very few studies that

426   report high-temporal frequency data of CH_4 emissions, most of which include plants within their

427   scope (via transparent chambers or eddy covariance) or focus on tidal creeks, making it difficult

428   to ascertain whether the diel patterns seen in this study are typical of tidal salt marsh soils. Of the

429   studies that report high-temporal frequency data of plant or water-based CH_4 fluxes in coastal

430   vegetated ecosystems, CH_4 emissions have been found to peak at various points in the day, from

431   during the day (Yang et al., 2018, 2017; Tong et al., 2013), at night (Diefenderfer et al., 2018), or

432   highly variable (Jha et al., 2014; Xu et al., 2017). At our site, CH_4 fluxes tended to peak at the

433   confluence of peak daily temperature and low to rising tides, indicating that physical forcing may

434   contribute to CH_4 pulses (Bahlmann et al., 2015; Middelburg et al., 1996). However, pulses did

435   occur during other times throughout the day and within the tidal cycle. While some of the pulse

436   emissions may be a result of ebullition, the majority are associated with high R^2's, indicating that

437   they are sustained over the measurement period. Our results demonstrate the importance of

438   conducting high-temporal frequency CH_4 measurements in tidal salt marsh soils for several

439 reasons, including the need for more data to better understand the drivers of CH_4 fluxes at diel

440 scales and how that affects model predictions.

441 N_2O emissions and uptake loosely followed a seasonal pattern, likely driven by the

442 canopy phenological stages. During the growing season, it has been shown that highly

443 productive plants can compete with soil microbes for NO_3^- and NH_4^- (Cheng et al., 2007; Yu et

444 al., 2012; Zhang et al., 2013; Granville et al., 2021; Xu et al., 2017), shifting denitrifiers into

445 consuming N_2O and resulting in a net uptake during G1 and M1. As the plants reach peak

446 maturity, the system shifts into net emission of N_2O during M2 and S1. One study found that

447 nitrogen additions resulted in a pulse of N_2O in July when most of the plant growth had occurred,

448 but no response in April, suggesting that the competition for NO_3^- and NH_3^+ decreases when

449 plant growth has slowed down (Moseman-Valtierra et al., 2011). Increased substrate availability

450 combined with warm temperatures likely contributed to the marsh being a net source of N_2O

451 during the later stages of the growing season. As temperatures drop, the system shifts back into

452 net uptake, as seen during S2 and D1. Similar seasonal patterns have been seen in other studies,

453 albeit shifted by a month or two depending on the local climate and phenophases (Granville et

454 al., 2021; Emery and Fulweiler, 2014). These findings highlight balance between processes that

455 produce N_2O (e.g., nitrification, denitrification, and nitrifier-denitrification) and consume N_2O

456 (e.g., denitrification), as well as substrate availability and plant phenology in determining

457 whether a marsh is a source or sink of N_2O at any given point.

458 As with seasonality, diel patterns of N_2O showed both emissions and uptake. Several

459 studies have also reported both emissions and uptake during a 24-hour period (Yang et al., 2017;

460 Tong et al., 2013). We found that pulses of uptake and emissions occurred both during the day

461 and at night, as well as during different phases of the tidal cycle. Studies have found higher

462   fluxes during the day (Tong et al., 2013; Yang et al., 2017) and at night (Laursen and Seitzinger,

463   2002; Yang et al., 2017; Bauza et al., 2002). Generally, fluxes were slightly higher at night

464   throughout the campaigns, perhaps as a result of increased availability of NH_4^+ at night due

465   decreased competition from photosynthesizers (Bauza et al., 2002). Overall, N_2O fluxes were

466   near-zero with a < 0.50 nmol m^{-2} s^{-1} difference between daytime and nighttime mean fluxes,

467   suggesting that N_2O fluxes do not play a major role in GHG emissions at this salt marsh.

468   Our automated measurements of sulfur-based trace gases show high variability in CS_2,

469   with low fluxes punctuated by occasional pulse emissions. There are no previous studies with

470   automated measurements to compare our findings, but previous studies have noted that CS_2

471   fluxes are highly variable (Steudler and Peterson, 1985; Hines, 1996), with periods of emission

472   and uptake. However, fluxes at SS were, on average, an order of magnitude higher than values

473   reported in the literature (Supplementary Table 1). There could be several reasons for the

474   difference in magnitudes: 1) improvement in instrumentation to detect CS_2, 2.) sampling

475   technique differences, and 3.) site-specific characteristics. Since the influx of sulfur-based trace

476   gas measurements in the 1980s, instrumentation has advanced from using molecular sieves and

477   cryotraps to store samples before measuring them on a gas chromatograph (e.g., Carroll et al.,

478   1986; Cooper et al., 1987; Steudler and Peterson, 1984) to using portable Fourier transform

479   infrared (FTIR) spectrometers that measure trace gas concentrations in near real-time. These

480   instrumentation advances subsequently led to changes in sampling techniques. Traditionally, it

481   was common to keep the chamber closed for upwards of 24-hours, with samples being collected

482   over hourly intervals throughout the day (Carroll et al., 1986; Goldan et al., 1987). Sweep air

483   free of sulfur trace gases was also commonly used to avoid the need to take samples at both the

484   inlet and outlets of the chambers (Goldan et al., 1987). However, others used ambient air because

485   it more closely resembled *in situ* conditions (Steudler and Peterson, 1985). With recent advances,

486   sampling techniques have changed to eliminate the need for very long closure times and reduce

487   the effects the chambers have on micrometeorological conditions. Now, high-temporal

488   frequency, long-term data can be obtained, thereby capturing pulse emissions that otherwise may

489   be missed. The third reason for difference in magnitude could be due to site-specific differences

490   in CS_2 fluxes. While the mechanisms by which CS_2 is produced are poorly understood, there are

491   several potential production pathways: OM degradation, photochemical production, and algal

492   production (Xie and Moore, 1999). The most likely pathway for our site is the microbially-

493   mediated reaction between H_2S and organic matter due to high sulfur concentrations, anaerobic

494   conditions, and a large pool of decaying organic matter. Finally, CS_2 is a short-lived sulfur gas

495   but the major product of CS_2 oxidation is COS; consequently, understanding CS_2 production and

496   oxidation is important for recognizing the role of salt marshes in COS dynamics (Whelan et al.,

497   2013).

498   The mean of measured DMS fluxes generally fall within those reported in the literature,

499   but with pulses higher than previously reported and different temporal patterns. We found that

500   DMS fluxes only occurred during the middle of the day, near when air temperatures peaked. This

501   is contrary to several studies that have found DMS fluxes during other times of the day

502   (Morrison and Hines, 1990; Steudler and Peterson, 1985; DeLaune et al., 2002). Some studies

503   have found diel patterns related to temperature (De Mello et al., 1987; Cooper et al., 1987b) and

504   incoming tides (Morrison and Hines, 1990; Dacey et al., 1987; Goldan et al., 1987). Our results

505   indicate that DMS fluxes from the SS site are associated with temperature and light-related

506   processes, whether these variables influence microbial activity, plant physiology, or a

507   combination of both. A study found that DMS fluxes peaked after a full daylight period in a

508   Danish estuary (Jørgensen and Okholm-Hansen, 1985). However, there is no information on the

509   diel patterns of DMS in the sediment pore water or its release from *S. alterniflora* plants. DMS is

510   also produced by other pathways that occur under anoxic conditions, such as methylation of

511   sulfide and methanethiol (Lomans et al., 2002; Sela-Adler et al., 2015), microbial reduction of

512   dimethylsulfoxide (Capone and Kiene, 1988), and/or the incorporation of inorganic substrates

513   (i.e., CO_2) and organic methylated compounds (Finster et al., 1990; Moran et al., 2008; Lin et al.,

514   2010). To better understand DMS fluxes, more research into the dynamics between *S.*

515   *alterniflora*, pore water DMS, and DMS fluxes is needed, as it plays an important role in carbon-

516   sulfur biogeochemistry, particularly as a non-competitive substrate for methylotrophic

517   methanogenesis (Seyfferth et al., 2020) .

518

519   *4.2 Continuous versus discrete measurements: do we get the same information?*

520   Our results show that discrete temporal measurements of CO_2 during daytime low tide

521   throughout the year (including dormancy) may be sufficient to obtain a representative mean of

522   the temporal variability of soil CO_2 flux. This has implications for calculating carbon budgets.

523   Furthermore, the distribution of continuous and discrete CO_2 fluxes is similar, indicating that

524   discrete measurements are capturing similar variability as continuous measurements. This

525   observation is reinforced by the $CO_2 \sim$ air temperature relationships, which do not have

526   significantly different slopes (discrete: 0.03 - 0.12, continuous: 0.04 - 0.05), providing further

527   support for the utility of daytime low tide discrete measurements in evaluating potential drivers

528   of CO_2 variability.

529   In contrast, high variability in CH_4 fluxes resulted in the means for discrete and

530   continuous measurements to be similar, but with significantly different distributions. In salt

531   marshes, CH_4 fluxes are characterized by high variability (Rosentreter et al., 2021), making it

532   difficult to assess the processes that control CH_4 fluxes (Vázquez-Lule and Vargas, 2021). While

533   the means were not significantly different despite ~33% higher mean flux using discrete

534   measurements, it is important to note that the 95% confidence interval and the coefficient of

535   variation are broad and very high, resulting in potential error cancellation for the calculation of

536   the mean. We postulate that the discrete measurement approach can be used to calculate budgets

537   with the caveat of large uncertainties and that they likely overestimate the mean CH_4 flux.

538   Discrete measurements do not capture similar variability as the continuous measurements and

539   have a stronger air temperature-CH_4 flux relationship than continuous measurements, despite the

540   overlap between their confidence intervals (2.14 - 12.7 and 1.31 - 2.71, respectively). However,

541   continuous measurements provide a more accurate depiction of the patterns and magnitudes of

542   CH_4 and can provide stronger insights into the interrelated drivers of CH_4 fluxes.

543   Regardless of the sampling interval, N_2O fluxes had means that are near-zero. Due to

544   fluxes consistently being near zero, the discrete and continuous measurements will likely get

545   similar overall results due to error cancellation even if the distributions were significantly

546   different. The continuous measurements capture a wider range of fluxes than the discrete

547   measurements, as seen with its very high coefficient of variance and a different distribution.

548   However, the skewness between the two approaches is very similar, due to the bulk of the

549   measurements falling around the same values as seen in the large amount of overlap in the

550   density curves. It is important to note that this site is nitrogen-limited, which constrains N_2O

551   production. In marshes that are not nitrogen-limited, sampling intervals will likely play a more

552   important role since fluxes will be higher.

553   For CS_2, discrete and continuous measurements did not have similar means or

554   distributions, likely due to the high variability found in these measurements. Previous studies

555   using discrete measurements of CS_2 have noted its high variability (e.g. De Mello et al., 1987),

556   with one highlighting the need for frequent measurements of sulfur-based trace gases during the

557   day in order to obtain an accurate mean daily flux value (Steudler and Peterson, 1985). We found

558   that discrete measurements taken during daytime low tide result in a daily mean that is nearly

559   twice that of the daily mean from the continuous measurements. The average CS_2 fluxes

560   measured during our field campaigns were up to an order of magnitude higher than previously

561   reported. We advocate for more measurements of CS_2 fluxes beyond focusing on low tide

562   windows and during different canopy phenological phases across salt marshes to better

563   understand the dynamics of this trace gas.

564   When measuring DMS fluxes during daytime low tide, the mean is similar to the

565   continuous measurement mean, but the distributions are significantly different. However, caution

566   should be taken in using discrete measurements of DMS to calculate daily means, particularly if

567   those measurements fall during the warmest part of the day when DMS fluxes are the most

568   active. This could result in overestimating the daily mean since extended periods of no fluxes are

569   not accounted for. One approach to measuring DMS fluxes would be to use the strong

570   relationship between discrete and continuous measurements to correct for the overestimation of

571   discrete fluxes. However, this approach would still require the use of a continuous, automated

572   system at different points throughout the year to establish a site-specific correction of discrete

573   mean DMS fluxes, particularly if DMS fluxes are used to calculate DMS budgets.

574

575   **5. Conclusion: what are we missing and challenges**

576   Discrete measurements have the clear advantage of capturing the spatial variability of soil

577   trace gas fluxes across an ecosystem, but this approach is also used to describe the temporal

578   variability. In contrast, continuous measurements using autochambers accurately describe

579   temporal patters (e.g., hourly measurements) but have limited spatial representation due to high

580   instrumentation costs and limited spatial extent of the area where autochambers can be deployed

581   (Vargas et al., 2011; Barba et al., 2018). Here we discuss the advantages and differences from

582   discrete and continuous measurements derived from this study. Discrete measurement campaigns

583   are suitable for calculating budgets, particularly for CO_2 and N_2O since they capture very similar

584   means but not the temporal variability. While we found that CH_4 and DMS means were not

585   significantly different between the two approaches, there are caveats that must be considered

586   when using discrete measurements. The high variability inherent in CH_4 fluxes can contribute to

587   the lack of significant differences between the two approaches and result in discrete

588   measurements overestimating the overall CH_4 fluxes from a tidal salt marsh. This has

589   implications when calculating SWGP where differences in CH_4 means largely contribute to the

590   differences in SGWP between the two approaches and can affect how scientists and

591   policymakers view tidal salt marshes and blue carbon as a natural climate solution (Macreadie et

592   al., 2021). For DMS, it is important to assess diel patterns to ensure that fluxes are

593   representative, particularly at sites that have patterns similar to what is seen at our study site.

594   When evaluating variability or trying to parse out the processes that drive GHG and trace gas

595   emissions from tidal salt marshes, using continuous, automated measurements would be the best

596   approach. This is particularly important for CH_4, where pulse emissions are frequent during the

597   growing season and can be very high. Using continuous measurements is also important in

598   scenarios where discrete measurements do not capture a similar mean or distribution, as with CS_2

599   fluxes. However, discrete measurements are more capable of representing spatial variability, and

600   until we have a better understanding of which source of variability is higher, temporal or spatial,

601   both techniques should be considered for ecosystem assessments.

602

603   **Data availability**

604   Meteorological (station: delsjmet-p) and water quality (station: Aspen Landing) data are

605   available from the National Estuarine Research Reserve's Centralized Data Management Office

606   (CDMO) at https://cdmo.baruch.sc.edu/. Phenological data are available from the PhenoCam

607   network (site: stjones) at https://phenocam.sr.unh.edu/webcam/sites/stjones/. Data from trace gas

608   fluxes are available in Figshare (doi:10.6084/m9.figshare.20449131).

609

610   **Author contributions**

611   MC and RV conceptualized the study, designed the methodology, and conducted project

612   administration. MC conducted the formal analysis, investigation, and visualization, as well as

613   wrote the original draft. RV provide funding, resources, supervision, as well as reviewed and

614   edited the manuscript.

615

616   **Competing interests**

617   The authors declare that they have no conflict of interest.

618

619

620   **Acknowledgments**

621   This research was supported by the National Science Foundation (#1652594). MC acknowledges

622   support from an NSF Graduate Research Fellowship (#1247394). We thank the onsite support

623   from Kari St. Laurent and the Delaware National Estuarine Research Reserve (DNERR), as well

624   as from Victor and Evelyn Capooci for field assistance during the first campaign. We thank

625   George Luther for inspiring discussions about carbon-sulfur biogeochemistry in salt marshes.

626   The authors acknowledge the land on which they conducted this study is the traditional home of

627   the Lenni-Lenape tribal nation (Delaware nation).

References

Al-Haj, A. N. and Fulweiler, R. W.: A synthesis of methane emissions from shallow vegetated coastal ecosystems, Glob. Chang. Biol., 26, 2988–3005, https://doi.org/10.1111/gcb.15046, 2020.

Andreae, M. O. and Jaeschke, W. A.: Exchange of sulfur between biosphere and atmosphere over temperate and tropical regions, in: Sulfur Cycling on the Continents, edited by: Howarth, R. W., Stewart, J. W. B., and Ivanov, M. V., Wiley, New York, 1992.

Bahlmann, E., Weinberg, I., Lavrič, J. V, Eckhardt, T., Michaelis, W., Santos, R., and Seifert, R.: Tidal controls on trace gas dynamics in a seagrass meadow of the Ria Formosa lagoon (southern Portugal), 12, 1683–1696, https://doi.org/10.5194/bg-12-1683-2015, 2015.

Barba, J., Cueva, A., Bahn, M., Barron-Gafford, G. A., Bond-Lamberty, B., Hanson, P. J., Jaimes, A., Kulmala, L., Pumpanen, J., Scott, R. L., Wohlfahrt, G., and Vargas, R.: Comparing ecosystem and soil respiration: Review and key challenges of tower-based and soil measurements, Agric. For. Meteorol., 249, 434–443, https://doi.org/10.1016/j.agrformet.2017.10.028, 2018.

Barbier, E., Hacker, S., Kennedy, C., Stier, A., and Silliman, B.: The value of estuarine and coastal ecosystem services, Ecol. Monogr., 81, 169–193, 2011.

Bartlett, K. B., Harriss, R. C., and Sebacher, D. I.: Methane Flux from Coastal Salt Marshes, J. Geophys. Res., 90, 5710–5720, 1985.

Bauza, J. F., Morell, J. M., and Corredor, J. E.: Biogeochemistry of nitrous oxide production in the red mangrove (Rhizophora mangle) forest sediments, Estuar. Coast. Shelf Sci., 55, 697–704, https://doi.org/10.1006/ecss.2001.0913, 2002.

Bridgham, S. D. and Richardson, C. J.: Mechanisms controlling soil respiration (CO2 and CH4) in southern peatlands, Soil Biol. Biochem., 24, 1089–1099, https://doi.org/10.1016/0038-0717(92)90058-6, 1992.

Brühl, C., Lelieveld, J., Crutzen, P. J., and Tost, H.: The role of carbonyl sulphide as a source of stratospheric sulphate aerosol and its impact on climate, Atmos. Chem. Phys., 12, 1239–1253, https://doi.org/10.5194/acp-12-1239-2012, 2012.

Capone, D. G. and Kiene, R. P.: Comparison of microbial dynamics in marine and freshwater sediment, Limnol. Ocean., 33, 725–749, 1988.

Capooci, M. and Vargas, R.: Diel and seasonal patterns of soil CO2 efflux in a temperate tidal marsh, Sci. Total Environ., 802, https://doi.org/10.1016/j.scitotenv.2021.149715, 2022.

Capooci, M., Barba, J., Seyfferth, A. L., and Vargas, R.: Experimental influence of storm-surge salinity on soil greenhouse gas emissions from a tidal salt marsh, Sci. Total Environ., 686, 1164–1172, https://doi.org/10.1016/j.scitotenv.2019.06.032, 2019.

Carroll, M. A., Heidt, L. E., Cicerone, R. J., and Prinn, R. G.: OCS, H2S, and CS2 fluxes from a salt water marsh, J. Atmos. Chem., 4, 375–395, https://doi.org/10.1007/BF00053811, 1986.

Charlson, R. J., Lovelock, J. E., Andreae, M. O., and Warren, S. G.: Oceanic phytoplankton, atmospheric sulphur, cloud albedo and climate, Nature, 326, 655–661, https://doi.org/10.1038/326655a0, 1987.

Cheng, X., Peng, R., Chen, J., Luo, Y., Zhang, Q., An, S., Chen, J., and Li, B.: CH4 and N2O emissions from Spartina alterniflora and Phragmites australis in experimental mesocosms, Chemosphere, 68, 420–427, https://doi.org/10.1016/J.CHEMOSPHERE.2007.01.004, 2007.

Cooper, D. J., De Mello, W. Z., Cooper, W. J., Zika, R. G., Saltzman, E. S., Prospero, J. M., and Savoie, D. L.: Short-term variability in biogenic sulphur emissions from a Florida Spartina alterniflora marsh, Atmos. Environ., 21, 7–12, 1987a.

Cooper, W. J., Cooper, D. J., Saltzman, E. S., Mello, W. Z. d., Savoie, D. L., Zika, R. G., and Prospero, J. M.: Emissions of biogenic sulphur compounds from several wetland soils in Florida, Atmos. Environ., 21, 1491–1495, https://doi.org/10.1016/0004-6981(87)90311-8, 1987b.

Dacey, J. W. H., King, G. M., and Wakeham, S. G.: Factors controlling emission of dimethylsulphide from salt marshes, Nature, 330, 643–645, https://doi.org/10.1038/330643a0, 1987.

DeLaune, R. D., Devai, I., and Lindau, C. W.: Flux of reduced sulfur gases along a salinity gradient in Louisiana coastal marshes, Estuar. Coast. Shelf Sci., 54, 1003–1011, https://doi.org/10.1006/ecss.2001.0871, 2002.

Diefenderfer, H. L., Cullinan, V. I., Borde, A. B., Gunn, C. M., and Thom, R. M.: High-frequency greenhouse gas flux measurement system detects winter storm surge effects on salt marsh, Glob. Chang. Biol., 24, 5961–5971, https://doi.org/10.1111/gcb.14430, 2018.

DNREC: Delaware National Esturaine Research Reserve Estuarine Profile, 158 pp., 1999.

Duarte, C. M., Middelburg, J. J., and Caraco, N.: Major role of marine vegetation on the oceanic carbon cycle, 2, 1–8, https://doi.org/10.1111/j.2042-7158.1975.tb10261.x, 2005.

Emery, H. E. and Fulweiler, R. W.: Spartina alterniflora and invasive Phragmites australis stands have similar greenhouse gas emissions in a New England marsh, Aquat. Bot., 116, 83–92, https://doi.org/10.1016/j.aquabot.2014.01.010, 2014.

Emmer, I., Needelman, B., Emmett-Mattox, S., Crooks, S., Beers, L., Megonigal, P., Myers, D., Oreska, M., McGlathery, K., and Shoch, D.: Methodology for Tidal Wetland and Seagrass Restoration, 1–115 pp., 2021.

Filippa, G., Cremonese, E., Migliavacca, M., Galvagno, M., Folker, M., Richardson, A. D., and Tomelleri, E.: phenopix: Process Digital Images of a Vegetation Cover, R Packag. version 2.4.2, 2020.

Finster, K., King, G. M., Bak, F., and Finster, K.: Formation of methylmercaptan and dimethylsulfide from methoxylated aromatic compounds in anoxic marine and fresh water sediments, FEMS Microbiol. Ecol., 74, 295–302, https://doi.org/10.1111/j.1574-6968.1990.tb04076.x, 1990.

Goldan, P. D., Kuster, W. C., Albritton, D. L., and Fehsenfeld, F. C.: The measurement of natural sulfur emissions from soils and vegetation: Three sites in the Eastern United States revisited, J. Atmos. Chem., 5, 439–467, https://doi.org/10.1007/BF00113905, 1987.

Granville, K. E., Ooi, S. K., Koenig, L. E., Lawrence, B. A., Elphick, C. S., and Helton, A. M.: Seasonal Patterns of Denitrification and N2O Production in a Southern New England Salt Marsh, 41, 1–13, https://doi.org/10.1007/s13157-021-01393-x, 2021.

Hill, A. C. and Vargas, R.: Methane and Carbon Dioxide Fluxes in a Temperate Tidal Salt Marsh: Comparisons Between Plot and Ecosystem Measurements, J. Geophys. Res. Biogeosciences, 127, e2022JG006943, https://doi.org/10.1029/2022JG006943, 2022.

Hill, A. C., Vázquez-Lule, A., and Vargas, R.: Linking vegetation spectral reflectance with ecosystem carbon phenology in a temperate salt marsh, Agric. For. Meteorol., 307, 108481, https://doi.org/10.1016/j.agrformet.2021.108481, 2021.

Hines, M. E.: Emissions of sulfur gases from wetlands, 25, 153–161, https://doi.org/10.1080/05384680.1996.11904076, 1996.

Järveoja, J., Nilsson, M. B., Gažovič, M., Crill, P. M., and Peichl, M.: Partitioning of the net CO2 exchange using an automated chamber system reveals plant phenology as key control of production and respiration fluxes in a boreal peatland, Glob. Chang. Biol., 24, 3436–3451, https://doi.org/10.1111/gcb.14292, 2018.

Jha, C. S., Rodda, S. R., Thumaty, K. C., Raha, A. K., and Dadhwal, V. K.: Eddy covariance based methane flux in Sundarbans mangroves, India, J. Earth Syst. Sci., 123, 1089–1096, https://doi.org/10.1007/s12040-014-0451-y, 2014.

Jørgensen, B. B. and Okholm-Hansen, B.: Emissions of biogenic sulfur gases from a danish estuary, Atmos. Environ., 19, 1737–1749, https://doi.org/10.1016/0004-6981(85)90001-0, 1985.

Kellogg, W. W., Cadle, R. D., Allen, E. R., Lazrus, A. L., and Martell, E. A.: The Sulfur Cycle, Science (80-.)., 175, 587–596, https://doi.org/10.1016/S0074-6142(08)62696-0, 1972.

Kiene, R. P.: Dimethyl sulfide metabolism in salt marsh sediments, FEMS Microbiol. Lett., 53, 71–78, https://doi.org/10.1016/0378-1097(88)90014-6, 1988.

737   Kiene, R. P. and Visscher, P. T.: Production and fate of methylated sulfur mompounds from
738   methionine and dimethylsulfoniopropionate in anoxic salt marsh sediments, Appl.
739   Environ. Microbiol., 53, 2426–2434, 1987.

740   Kim, J., Verma, S. B., Billesbach, D. P., and Clement, R. J.: Diel variation in methane emission
741   from a midlatitude prairie wetland: Significance of convective throughflow in
742   Phragmites australis, J. Geophys. Res. Atmos., 103, 28029–28039,
743   https://doi.org/10.1029/98JD02441, 1998.

744   Koskinen, M., Minkkinen, K., Ojanen, P., Kämäräinen, M., Laurila, T., and Lohila, A.:
745   Measurements of CO2 exchange with an automated chamber system throughout the
746   year: Challenges in measuring night-time respiration on porous peat soil, 11, 347–363,
747   https://doi.org/10.5194/bg-11-347-2014, 2014.

748   Laursen, A. E. and Seitzinger, S. P.: Measurement of denitrification in rivers: an integrated,
749   whole reach approach, Hydrobiologia, 485, 67–81, 2002.

750   Lin, Y. S., Heuer, V. B., Ferdelman, T. G., and Hinrichs, K.-U.: Microbial conversion of
751   inorganic carbon to dimethyl sulfide in anoxic lake sediment (Plußsee, Germany), 7,
752   2433–2444, https://doi.org/10.5194/bg-7-2433-2010, 2010.

753   Livesley, S. J. and Andrusiak, S. M.: Temperate mangrove and salt marsh sediments are a small
754   methane and nitrous oxide source but important carbon store, Estuar. Coast. Shelf Sci.,
755   97, 19–27, https://doi.org/10.1016/j.ecss.2011.11.002, 2012.

756   Lomans, B. P., Van der Drift, C., Pol, A., and Op den Camp, H. J. M.: Microbial cycling of
757   volatile organic sulfur compounds, Water Sci. Technol., 45, 55–60,
758   https://doi.org/10.1007/s00018-002-8450-6, 2002.

759   Macreadie, P. I., Costa, M. D. P., Atwood, T. B., Friess, D. A., Kelleway, J. J., Kennedy, H.,
760   Lovelock, C. E., Serrano, O., and Duarte, C. M.: Blue carbon as a natural climate
761   solution, Nat. Rev. Earth Environ., 2, 826–839,
762   https://doi.org/https://doi.org/10.1038/s43017-021-00224-1, 2021.

763   McTigue, N. D., Walker, Q. A., and Currin, C. A.: Refining Estimates of Greenhouse Gas
764   Emissions From Salt Marsh "Blue Carbon" Erosion and Decomposition, Front. Mar.
765   Sci., 8, 1–13, https://doi.org/10.3389/fmars.2021.661442, 2021.

766   De Mello, W. Z., Cooper, D. J., Cooper, W. J., Saltzman, E. S., Zika, R. G., Savoie, D. L., and
767   Prospero, J. M.: Spatial and diel variability in the emissions of some biogenic sulfur
768   compounds from a Florida Spartina alterniflora coastal zone, Atmos. Environ., 21, 987–
769   990, https://doi.org/10.1016/0004-6981(87)90095-3, 1987.

770   Middelburg, J. J., Klaver, G., Nieuwenhuize, J., Wielemaker, A., de Hass, W., Vlug, T., and
771   van der Nat, J. F. W. A.: Organic matter mineral sediments along an estuarine gradient,
772   Mar. Ecol. Prog. Ser., 132, 157–168, 1996.

773   Moffett, K. B., Wolf, A., Berry, J. A., and Gorelick, S. M.: Salt marsh-atmosphere exchange of

774   energy, water vapor, and carbon dioxide: Effects of tidal flooding and biophysical
775   controls, 46, https://doi.org/10.1029/2009WR009041, 2010.

776 Möller, I., Kudella, M., Rupprecht, F., Spencer, T., Paul, M., Van Wesenbeeck, B. K., Wolters,
777   G., Jensen, K., Bouma, T. J., Miranda-Lange, M., and Schimmels, S.: Wave attenuation
778   over coastal salt marshes under storm surge conditions, Nat. Geosci., 7, 727–731,
779   https://doi.org/10.1038/NGEO2251, 2014.

780 Moran, J. J., House, C. H., Vrentas, J. M., and Freeman, K. H.: Methyl sulfide production by a
781   novel carbon monoxide metabolism in Methanosarcina acetivorans, Appl. Environ.
782   Microbiol., 74, 540–542, https://doi.org/10.1128/AEM.01750-07, 2008.

783 Morrison, M. C. and Hines, M. E.: The variability of biogenic sulfur flux from a temperate salt
784   marsh on short time and space scales, Atmos. Environ. Part A. Gen. Top., 24A, 1771–
785   1779, https://doi.org/10.1016/0960-1686(90)90509-L, 1990.

786 Moseman-Valtierra, S., Gonzalez, R., Kroeger, K. D., Tang, J., Chao, W. C., Crusius, J.,
787   Bratton, J., Green, A., and Shelton, J.: Short-term nitrogen additions can shift a coastal
788   wetland from a sink to a source of N2O, Atmos. Environ., 45, 4390–4397,
789   https://doi.org/10.1016/j.atmosenv.2011.05.046, 2011.

790 Moseman-Valtierra, S., Abdul-Aziz, O. I., Tang, J., Ishtiaq, K. S., Morkeski, K., Mora, J.,
791   Quinn, R. K., Martin, R. M., Egan, K., Brannon, E. Q., Carey, J., and Kroeger, K. D.:
792   Carbon dioxide fluxes reflect plant zonation and belowground biomass in a coastal
793   marsh, 7, e01560, 2016.

794 Murray, R. H., Erler, D. V., and Eyre, B. D.: Nitrous oxide fluxes in estuarine environments :
795   response to global change, Glob. Chang. Biol., 21, 3219–3245,
796   https://doi.org/10.1111/gcb.12923, 2015.

797 Van Der Nat, F. and Middelburg, J. J.: Methane emission from tidal freshwater marshes,
798   Biogeochemistry, 49, 103–121, 2000.

799 Neubauer, S. C. and Megonigal, J. P.: Correction to: Moving Beyond Global Warming
800   Potentials to Quantify the Climatic Role of Ecosystems, Ecosyst. 2019 228, 22, 1931–
801   1932, https://doi.org/10.1007/S10021-019-00422-5, 2019.

802 System-wide Monitoring Program:

803 Oremland, R. S., Marsh, L. M., and Polcin, S.: Methane production and simultaneous sulphate
804   reduction in anoxic, salt marsh sediments, Nature, 296, 143–145, 1982.

805 Peterson, P. M., Romaschenko, K., Arrieta, Y. H., and Saarela, J. M.: A molecular phylogeny
806   and new subgeneric classification of Sporobolus (Poaceae: Chloridoideae:
807   Sporobolinae), Taxon, 63, 1212–1243, https://doi.org/10.12705/636.19, 2014.

808 Petrakis, S., Seyfferth, A., Kan, J., Inamdar, S., and Vargas, R.: Influence of experimental
809   extreme water pulses on greenhouse gas emissions from soils, Biogeochemistry, 133,

810   147–164, https://doi.org/10.1007/s10533-017-0320-2, 2017.

811   Rinne, J., Riutta, T., Pihlatie, M., Aurela, M., Haapanala, S., Tuovinen, J. P., Tuittila, E. S., and
812   Vesala, T.: Annual cycle of methane emission from a boreal fen measured by the eddy
813   covariance technique, Tellus, Ser. B Chem. Phys. Meteorol., 59, 449–457,
814   https://doi.org/10.1111/j.1600-0889.2007.00261.x, 2007.

815   Rosentreter, J. A., Maher, D. T., Erler, D. V., Murray, R. H., and Eyre, B. D.: Methane
816   emissions partially offset "blue carbon" burial in mangroves, Sci. Adv., 4, eaao4985,
817   https://doi.org/10.1126/SCIADV.AAO4985, 2018.

818   Rosentreter, J. A., Al-Haj, A. N., Fulweiler, R. W., and Williamson, P.: Methane and Nitrous
819   Oxide Emissions Complicate Coastal Blue Carbon Assessments, Global Biogeochem.
820   Cycles, 35, e2020GB006858, https://doi.org/10.1029/2020GB006858, 2021.

821   Savage, K., Phillips, R., and Davidson, E.: High temporal frequency measurements of
822   greenhouse gas emissions from soils, 11, 2709–2720, https://doi.org/10.5194/bg-11-
823   2709-2014, 2014.

824   Sela-Adler, M., Said-Ahmad, W., Sivan, O., Eckert, W., Kiene, R. P., and Amrani, A.: Isotopic
825   evidence for the origin of dimethylsulfide and dimethylsulfoniopropionate-like
826   compounds in a warm, monomictic freshwater lake, Environ. Chem., 13, 340–351,
827   https://doi.org/https://doi.org/10.1071/EN15042, 2015.

828   Seyednasrollah, B., Young, A. M., Hufkens, K., Milliman, T., Friedl, M. A., Frolking, S.,
829   Richardson, A. D., Abraha, M., Allen, D. W., Apple, M., Arain, M. A., Baker, J., Baker,
830   J. M., Baldocchi, D., Bernacchi, C. J., Bhattacharjee, J., Blanken, P., Bosch, D. D.,
831   Boughton, R., Boughton, E. H., and Zona, D.: PhenoCam dataset v2.0: Vegetation
832   phenology from digital camera imagery, Oak Ridge, Tennessee,
833   https://doi.org/https://doi.org/10.3334/ ORNLDAAC/1674, 2019.

834   Seyfferth, A. L., Bothfeld, F., Vargas, R., Stuckey, J. W., Wang, J., Kearns, K., Michael, H. A.,
835   Guimond, J., Yu, X., and Sparks, D. L.: Spatial and temporal heterogeneity of
836   geochemical controls on carbon cycling in a tidal salt marsh, Geochim. Cosmochim.
837   Acta, 282, 1–18, https://doi.org/10.1016/j.gca.2020.05.013, 2020.

838   Simpson, L. T., Osborne, T. Z., and Feller, I. C.: Wetland Soil CO2 Efflux Along a Latitudinal
839   Gradient of Spatial and Temporal Complexity, 42, 45–54,
840   https://doi.org/10.1007/s12237-018-0442-3, 2019.

841   Steudler, P. A. and Peterson, B. J.: Contribution of gaseous sulphur from salt marshes to the
842   global sulphur cycle, Nature, 311, 455–457, https://doi.org/10.1038/311455a0, 1984.

843   Steudler, P. A. and Peterson, B. J.: Annual cycle of gaseous sulfur emissions from a New
844   England Spartina alterniflora marsh, Atmos. Environ., 19, 1411–1416,
845   https://doi.org/10.1016/0004-6981(85)90278-1, 1985.

846   Taubman, S. J. and Kasting, J. F.: Carbonyl sulfide: No remedy for global warming, Geophys.

847   Res. Lett., 22, 803–805, https://doi.org/10.1029/95GL00636, 1995.

848   Thomas, M. A., Suntharalingam, P., Pozzoli, L., Rast, S., Devasthale, A., Kloster, S., Feichter,
849   J., and Lenton, T. M.: Quantification of DMS aerosol-cloud-climate interactions using
850   the ECHAM5-HAMMOZ model in a current climate scenario, Atmos. Chem. Phys., 10,
851   7425–7438, https://doi.org/10.5194/acp-10-7425-2010, 2010.

852   Tong, C., Huang, J. F., Hu, Z. Q., and Jin, Y. F.: Diurnal Variations of Carbon Dioxide,
853   Methane, and Nitrous Oxide Vertical Fluxes in a Subtropical Estuarine Marsh on Neap
854   and Spring Tide Days, 36, 633–642, https://doi.org/10.1007/s12237-013-9596-1, 2013.

855   Tong, C., Morris, J. T., Huang, J., Xu, H., and Wan, S.: Changes in pore-water chemistry and
856   methane emission following the invasion of Spartina alterniflora into an oliogohaline
857   marsh, Limnol. Oceanogr., 63, 384–396, https://doi.org/10.1002/lno.10637, 2018.

858   Trifunovic, B., Vázquez-Lule, A., Capooci, M., Seyfferth, A. L., Moffat, C., and Vargas, R.:
859   Carbon Dioxide and Methane Emissions From Temperate Salt Marsh Tidal Creek, J.
860   Geophys. Res. Biogeosciences, 125, https://doi.org/10.1029/2019JG005558, 2020.

861   Turetsky, M. R., Kotowska, A., Bubier, J., Dise, N. B., Crill, P., Hornibrook, E. R. C.,
862   Minkkinen, K., Moore, T. R., Myers-Smith, I. H., Nykanen, H., Olefeldt, D., Rinne, J.,
863   Saarnio, S., Shurpali, N., Tuittila, E. S., Waddington, J. M., White, J. R., Wickland, K.
864   P., and Wilmking, M.: A synthesis of methane emissions from 71 northern, temperate,
865   and subtropical wetlands, Glob. Chang. Biol., 20, 2183–2197,
866   https://doi.org/10.1111/gcb.12580, 2014.

867   UNFCCC: Paris Agreement, 2015.

868   Vargas, R., Carbone, M. S., Reichstein, M., and Baldocchi, D. D.: Frontiers and challenges in
869   soil respiration research: from measurements to model-data integration,
870   Biogeochemistry, 102, 1–13, https://doi.org/10.1007/s10533-010-9462-1, 2011.

871   Vázquez-Lule, A. and Vargas, R.: Biophysical drivers of net ecosystem and methane exchange
872   across phenological phases in a tidal salt marsh, Agric. For. Meteorol., 300,
873   https://doi.org/10.1016/j.agrformet.2020.108309, 2021.

874   Wang, J. and Wang, J.: Spartina alterniflora alters ecosystem DMS and CH4 emissions and
875   their relationship along interacting tidal and vegetation gradients within a coastal salt
876   marsh in Eastern China, Atmos. Environ., 167, 346–359,
877   https://doi.org/10.1016/J.ATMOSENV.2017.08.041, 2017.

878   Ward, N., Megonigal, P. J., Bond-Lamberty, B., Bailey, V., Butman, D., Canuel, E.,
879   Diefenderfer, H., Ganju, N. K., Goñi, M. A., Graham, E. B., Hopkinson, C. S.,
880   Khangaonkar, T., Langley, J. A., McDowell, N. G., Myers-Pigg, A. N., Neumann, R.
881   B., Osburn, C. L., Price, R. M., Rowland, J., Sengupta, A., Simard, M., Thornton, P. E.,
882   Tzortziou, M., Vargas, R., Weisenhorn, P. B., and Windham-Myers, L.: Representing
883   the Function and Sensitivity of Coastal Interfaces in Earth System Models, Nat.
884   Commun., 11, https://doi.org/10.1038/s41467-020-16236-2, 2020.

Watts, S. F.: The mass budgets of carbonyl sulfide, dimethyl sulfide, carbon disulfide and hydrogen sulfide, Atmos. Environ., 34, 761–779, https://doi.org/10.1016/S1352-2310(99)00342-8, 2000.

Whelan, M. E., Min, D. H., and Rhew, R. C.: Salt marsh vegetation as a carbonyl sulfide (COS) source to the atmosphere, Atmos. Environ., 73, 131–137, https://doi.org/10.1016/J.ATMOSENV.2013.02.048, 2013.

Wilson, B. J., Mortazavi, B., and Kiene, R. P.: Spatial and temporal variability in carbon dioxide and methane exchange at three coastal marshes along a salinity gradient in a northern Gulf of Mexico estuary, Biogeochemistry, 123, 329–347, https://doi.org/10.1007/s10533-015-0085-4, 2015.

Xie, H. and Moore, R. M.: Carbon disulfide in the North Atlantic and Pacific Oceans, J. Geophys. Res. Ocean., 104, 5393–5402, https://doi.org/10.1029/1998jc900074, 1999.

Xie, X., Zhang, M.-Q., Zhao, B., and Guo, H.-Q.: Dependence of coastal wetland ecosystem respiration on temperature and tides: a temporal perspective, 11, 539–545, https://doi.org/10.5194/bg-11-539-2014, 2014.

Xu, X., Fu, G., Zou, X., Ge, C., and Zhao, Y.: Diurnal variations of carbon dioxide, methane, and nitrous oxide fluxes from invasive Spartina alterniflora dominated coastal wetland in northern Jiangsu Province, Acta Oceanol. Sin., 36, 105–113, https://doi.org/10.1007/s13131-017-1015-1, 2017.

Yang, W.-B., Yuan, C.-S., Huang, B.-Q., Tong, C., and Yang, L.: Emission Characteristics of Greenhouse Gases and Their Correlation with Water Quality at an Estuarine Mangrove Ecosystem – the Application of an In-situ On-site NDIR Monitoring Technique, Wetl. 2018 384, 38, 723–738, https://doi.org/10.1007/S13157-018-1015-8, 2018.

Yang, W.-B. Bin, Yuan, C.-S. S., Tong, C., Yang, P., Yang, L., and Huang, B.-Q. Q.: Diurnal variation of CO2, CH4, and N2O emission fluxes continuously monitored in-situ in three environmental habitats in a subtropical estuarine wetland, Mar. Pollut. Bull., 119, 289–298, https://doi.org/10.1016/j.marpolbul.2017.04.005, 2017.

Yu, X., Ye, S., Olsson, L., Wei, M., Krauss, K. W., and Brix, H.: A 3-Year In-Situ Measurement of CO 2 Efflux in Coastal Wetlands: Understanding Carbon Loss through Ecosystem Respiration and its Partitioning, https://doi.org/10.1007/s13157-019-01197-0, 2019.

Yu, Z., Li, Y., Deng, H., Wang, D., Chen, Z., and Xu, S.: Effect of Scirpus mariqueter on nitrous oxide emissions from a subtropical monsoon estuarine wetland, J. Geophys. Res. Biogeosciences, 117, 2017, https://doi.org/10.1029/2011JG001850, 2012.

Zhang, Y. and Ding, W.: Diel methane emissions in stands of Spartina alterniflora and Suaeda salsa from a coastal salt marsh, Aquat. Bot., 95, 262–267, https://doi.org/10.1016/j.aquabot.2011.08.005, 2011.

922   Zhang, Y., Wang, L., Xie, X., Huang, L., and Wu, Y.: Effects of invasion of Spartina
923   alterniflora and exogenous N deposition on N2O emissions in a coastal salt marsh, Ecol.
924   Eng., 58, 77–83, https://doi.org/10.1016/j.ecoleng.2013.06.011, 2013.

925